

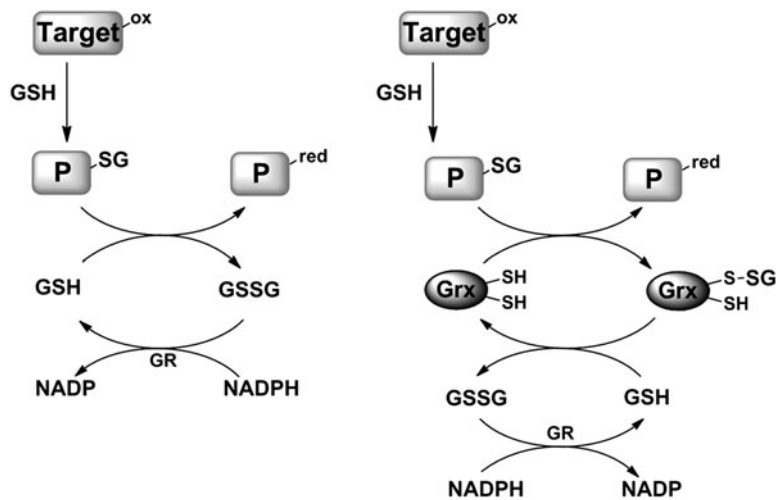
Supplementary Data

Supplementary Materials and Methods

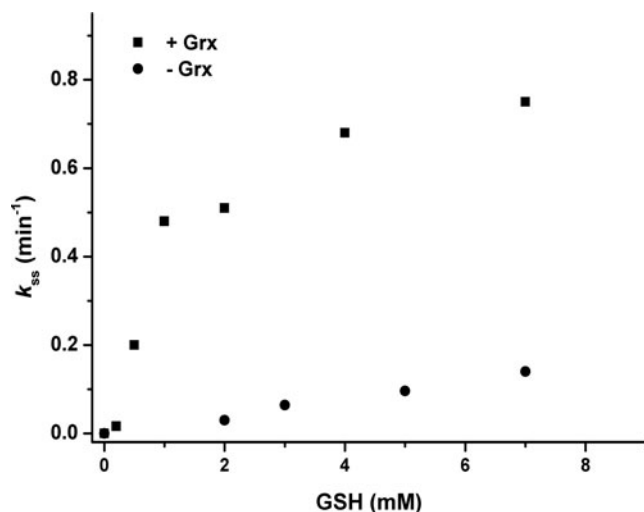
Production and purification of mouse *Srx* and *Prx1*

Recombinant *M. musculus* *Srx* was obtained by cloning a synthetic ORF coding mouse *Srx* optimized for expression in *Escherichia coli* (GeneArt; Life Technologies, Carlsbad, CA) into a modified pGEX-6P-1 plasmid (GE Healthcare Bio-Sciences, Piscataway, NJ), enabling production of an N-terminal 6xHis/GST fusion protein. Recombinant His-tagged mouse *Prx1* was obtained by cloning a synthetic ORF coding mouse *Prx1* optimized for expression in *E. coli* (GeneArt; Life Technologies) into the pET28b(+) plasmid (source) between the *Nde*I and *Sac*I sites. The C41(DE3) [*F*⁻ *ompT* *hsdS*_B (*r*_B⁻ *m*_B⁻) *gal dcm* (DE3)] *E. coli* strain was used for production of mouse *Srx* and *Prx1*.

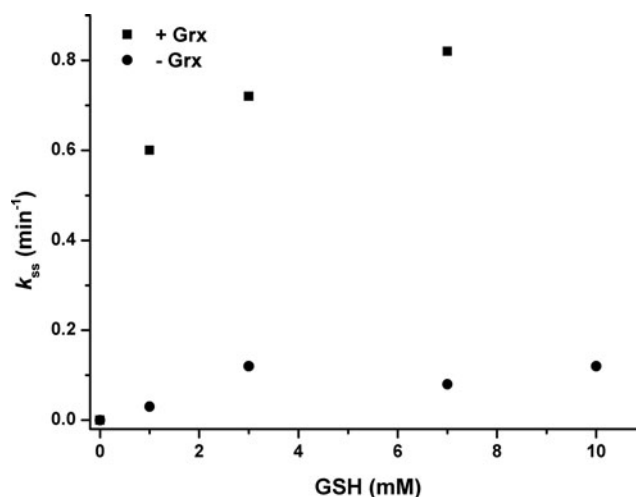
For protein purification, cells were harvested by centrifugation, resuspended in a minimal volume of buffer (50 mM potassium phosphate buffer, 50 mM imidazole, 0.5 M KCl, pH7) and sonicated. The fusion His tagged proteins contained in the soluble fraction were purified on an Ni-Sepharose column that was connected to an AKTA FPLC system (GE Healthcare Bio-Sciences), and eluted by a 0.5 M imidazole step. For mouse *Srx*, the HT-GST tag was cleaved by the PreScission protease (GE Healthcare Bio-Sciences) overnight at 4°C, before final purification by gel filtration on a superdex 75 column. Both purified proteins were stored at -20°C, in the presence of 15% glycerol and 10 mM DTT. Molecular concentrations were determined spectrophotometrically, using theoretical extinction coefficients at 280 nm of 13,400 M⁻¹.cm⁻¹ for mouse *Srx* and 20,065 M⁻¹.cm⁻¹ for mouse *Prx1*.



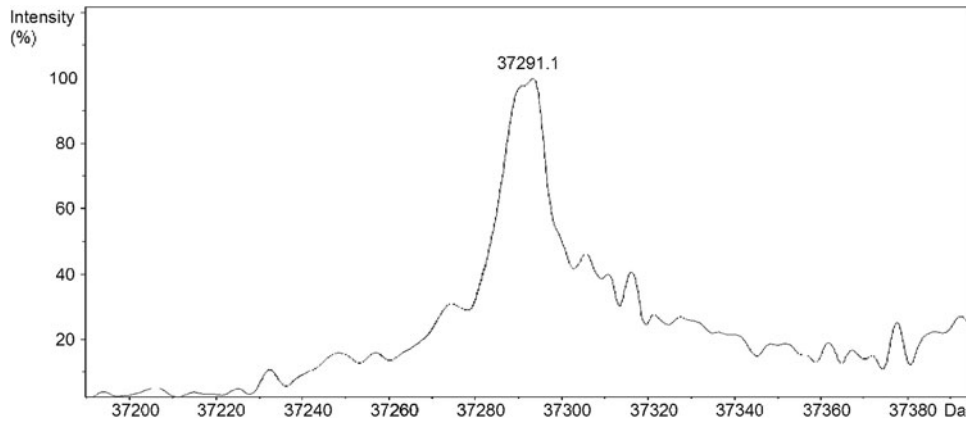
SUPPLEMENTARY FIG. S1. Schematic principle of the GSH/GR (left) and GSH/Grx/GR (right) coupled assays. The oxidized target is reduced by a molecule of GSH, which results in formation of a glutathionylated protein (P). The glutathionyl moiety is then transferred to a second GSH molecule either directly (left) or via Grx (right). The oxidized glutathione GSSG produced is reduced to GSH by GR coupled to NADPH oxidation. GR: glutathione reductase.



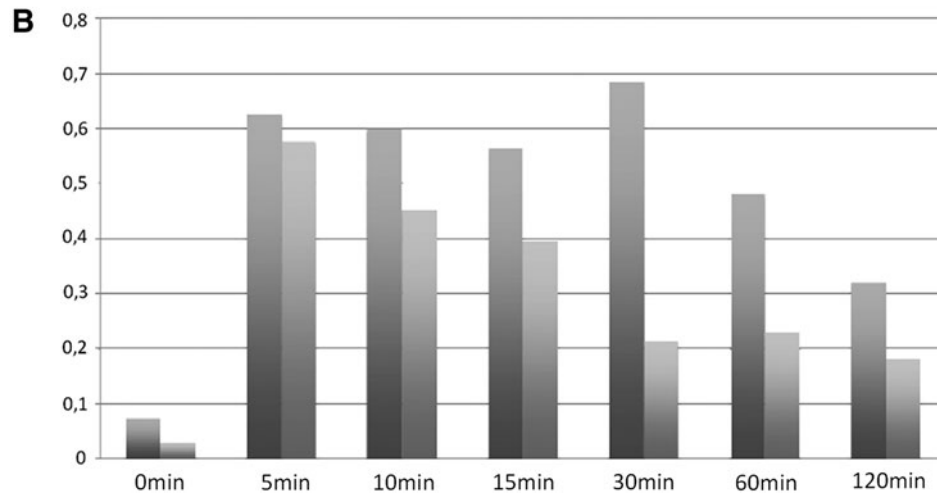
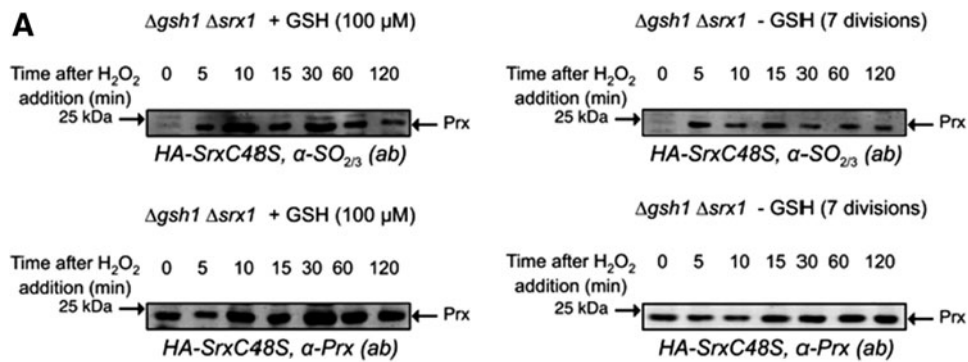
SUPPLEMENTARY FIG. S2. Steady-state kinetics of SrxC⁸⁴ using wild-type Prx-SO₂ substrate, recycled by the GSH/Grx/GR system. The reaction of 25 μ M Prx-SO₂ with 10 μ M SrxC⁸⁴ in the presence of 1 mM MgCl₂ was followed using the GSH/GR (0.5 μ M GR and 200 μ M NADPH, *circles*), GSH/Grx/GR (50 μ M Grx, 0.5 μ M GR, and 200 μ M NADPH, *squares*) coupled assay. The assay was initiated by the addition of 1 mM ATP. Initial rate measurements were carried out at 30°C in buffer TK by following the decrease in absorbance at 340 nm due to the oxidation of NADPH. The lower maximum rate constant of 0.8 versus 1.2 min⁻¹ obtained for C171A Prx-SO₂ is due to the use of a Prx-SO₂ concentration of 25 μ M, which is slightly sub-saturating relative to SrxC⁸⁴.



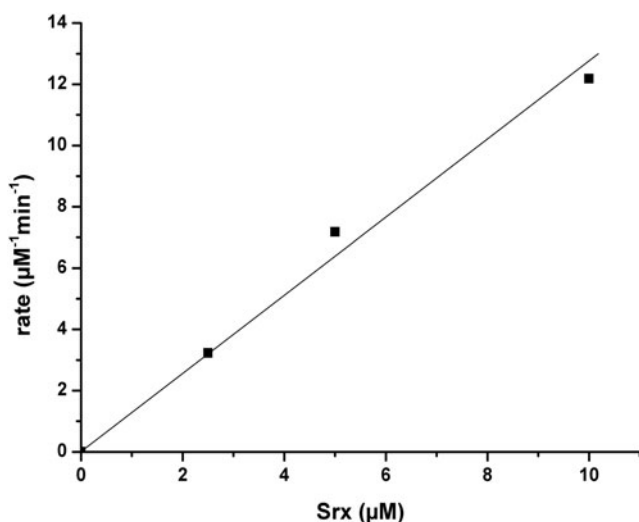
SUPPLEMENTARY FIG. S3. Mouse SrxC⁸⁴ is recycled by the GSH/Grx/GR system in the steady state. The reaction of 50 μ M mouse hyperoxidized Prx1 with 10 μ M mouse SrxC⁸⁴ in the presence of 1 mM MgCl₂ was followed using the GSH/GR (0.5 μ M GR and 200 μ M NADPH, *circles*), or GSH/Grx/GR (50 μ M *E. coli* Grx, 0.5 μ M GR, and 200 μ M NADPH, *squares*) coupled assays. The assay was started by addition of 1 mM ATP. Initial rate measurements were carried out at 30°C in buffer TK by following the decrease in absorbance at 340 nm due to the oxidation of NADPH.



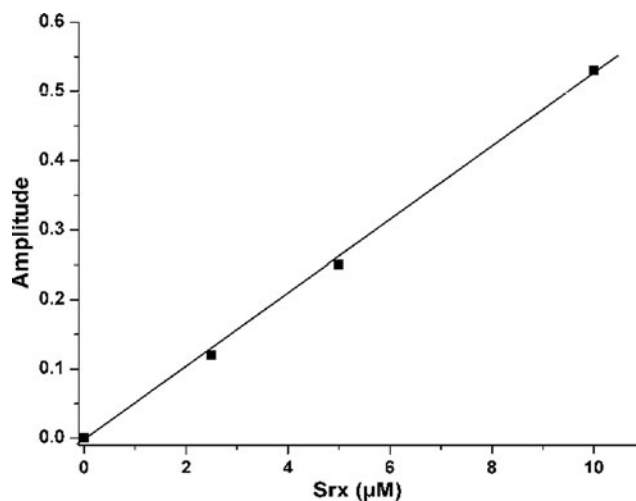
SUPPLEMENTARY FIG. S4. Mass spectrometry analysis of the Prx-Srx complex used in Figure 5A. Deconvoluted mass spectrum of the species eluting in peak **c** (Fig. 4A) after 1 min of incubation of equimolar concentrations ($30 \mu\text{M}$) of C171A Prx-SO₂ and Srx C84A-C106V (equivalent to Srx^{C84}) in the presence of 1 mM ATP and MgCl₂, in buffer TK at 30°C. Expected mass for the Prx-SO-S-Srx species: 37290.5 Da.



SUPPLEMENTARY FIG. S5. Impact of GSH on the kinetics of Prx-SO₂ reduction *in vivo*. (A) Cultures of *Δgsh1 Δsrx1* carrying pRS316-HA2-SrxC48S, grown in selective minimal medium (SD URA⁻) supplemented with 100 μM GSH (*left panels*), or grown for seven divisions in selective minimal medium (SD URA⁻) lacking GSH (*right panels*), were exposed during 30 min of 100 μM H₂O₂ to induce *SRX1* expression. After 30 min, cells were exposed again to 500 μM H₂O₂ and lysed after 5, 10, 15, 30, 60, and 120 min by the TCA protocol. Normalized total protein extracts were immunoblotted with anti-Prx-SO_{2/3} or anti-Prx (anti Tsa1) antibodies, after separation by reducing 15% SDS-PAGE. (B) The band intensities corresponding to Prx-SO₂ were normalized relative to total Prx, for cells grown in the presence (*light gray*) or absence (*dark gray*) of GSH.



SUPPLEMENTARY FIG. S6. The rate of the Srx-catalyzed reaction in steady state is proportional to Srx. The reaction of $50 \mu\text{M}$ Prx-SO₂ with 0, 2.5, 5, and $10 \mu\text{M}$ Srx^{C84} in the presence of 1 mM MgCl₂ was followed using the GSH/Grx/GR ($50 \mu\text{M}$ Grx, $0.5 \mu\text{M}$ GR, and $200 \mu\text{M}$ NADPH, *squares*) coupled assay in the presence of 1 mM GSH. The assay was started by the addition of 1 mM ATP. Initial rate measurements were carried out at 30°C in buffer TK by following the decrease in absorbance at 340 nm due to the oxidation of NADPH. The slope of the line corresponds to a steady-state rate constant k_{ss} of 1.2 min^{-1} .



SUPPLEMENTARY FIG. S7. Impact of Srx concentration on the kinetics of Srx reduction by GSH under single-turnover conditions. Final concentrations of $40 \mu\text{M}$ Prx-SO₂, 1 mM ATP, 1 mM MgCl₂, and 1 mM GSH were rapidly mixed with 0, 2.5, 5, and $10 \mu\text{M}$ Srx^{C84} in buffer TK at 30°C in a rapid kinetics spectrofluorometer. Quenching of fluorescence emission intensity of wild-type Prx on going from the oxidized Prx-SO₂ to the disulfide form was recorded on an SX18MV-R stopped-flow apparatus fitted for fluorescence measurements, with excitation wavelength set at 295 nm , and emitted light collected above 320 nm using a cutoff filter. The blank-corrected progress curves were analyzed using a first-order kinetic model to deduce the amplitudes (*squares*) of the process.